2016

Robust ferromagnetism of single crystalline CoxZn1−xO (0.3 ≤ x ≤ 0.45) epitaxial films with high Co concentration

Qiang Cao
Shandong University

Dapeng Zhu
Shandong University

Maxiang Fu
Shandong University

Li Cai
Shandong University

Ping Yang
National University of Singapore

See next page for additional authors

Publication Details

Cao, Q., Zhu, D., Fu, M., Cai, L., Yang, P., Li, S., Zhu, Y., Ma, X., Liu, G., Chen, Y., Yan, S., Mei, L. & Wang, X. (2016). Robust ferromagnetism of single crystalline CoxZn1−xO (0.3 ≤ x ≤ 0.45) epitaxial films with high Co concentration. Applied Physics Letters, 109 (5), 052404-1-052404-5.

Robust ferromagnetism of single crystalline CoxZn1−xO (0.3 ≤ x ≤ 0.45) epitaxial films with high Co concentration

Abstract
In contrast to conventional dilute magnetic semiconductors with concentrations of magnetic ions of just a few percent, here, we report the fabrication of epitaxial Cox Zn 1− xO single crystalline films with Co concentrations from x = 0.3 up to 0.45 by radio-frequency oxygen-plasma-assisted molecular beam epitaxy. The films retain their single crystalline wurtzite structure without any other crystallographic phase from precipitates, based on reflection high energy electron diffraction, X-ray diffraction, transmission electron microscopy, and Raman scattering. The results of X-ray diffraction, optical transmission spectroscopy, and in-situ X-ray photoelectron spectroscopy confirm the incorporation of Co2+ cations into the wurtzite lattice. The films exhibit robust ferromagnetism and the magneto-optical Kerr effect at room temperature. The saturation magnetization reaches 265 emu/cm3 at x = 0.45, which corresponds to the average magnetic moment of 1.5 μB per Co atom.

Disciplines
Engineering | Physical Sciences and Mathematics

Publication Details
Cao, Q., Zhu, D., Fu, M., Cai, L., Yang, P., Li, S., Zhu, Y., Ma, X., Liu, G., Chen, Y., Yan, S., Mei, L. & Wang, X. (2016). Robust ferromagnetism of single crystalline CoxZn1−xO (0.3 ≤ x ≤ 0.45) epitaxial films with high Co concentration. Applied Physics Letters, 109 (5), 052404-1-052404-5.

Authors
Qiang Cao, Dapeng Zhu, Maxiang Fu, Li Cai, Ping Yang, Shuang Li, Yinlian Zhu, Xiuliang Ma, Guo-Lei Liu, Yan-Xue Chen, Shi-Shen Yan, Liang-Mo Mei, and Xiaolin Wang

Robust ferromagnetism of single crystalline $Co_xZn_{1-x}O$ ($0.3 \le x \le 0.45$) epitaxial films with high Co concentration

Qiang Cao,[1,2,a)] Dapeng Zhu,[1] Maoxiang Fu,[1] Li Cai,[1] Ping Yang,[3] Shuang Li,[4] Yinlian Zhu,[4] Xiuliang Ma,[4] Guolei Liu,[1,a)] Yanxue Chen,[1] Shishen Yan,[1] Liangmo Mei,[1] and Xiaolin Wang[5]

[1]*School of Physics and National Key Laboratory of Crystal Materials, Shandong University, Jinan 250100, China*
[2]*School of Physics and Engineering, Qufu Normal University, Qufu 273165, China*
[3]*Singapore Synchrotron Light Source, National University of Singapore, 5 Research Link, Singapore 117603, Singapore*
[4]*Shenyang National Laboratory for Materials Science, Institute of Metal Research, Chinese Academy of Sciences, Shenyang 110016, China*
[5]*Institute for Superconducting and Electronic Materials, Australian Institute for Innovative Materials, University of Wollongong, Innovation Campus, North Wollongong, New South Wales 2500, Australia*

(Received 27 June 2016; accepted 26 July 2016; published online 4 August 2016)

In contrast to conventional dilute magnetic semiconductors with concentrations of magnetic ions of just a few percent, here, we report the fabrication of epitaxial $Co_xZn_{1-x}O$ single crystalline films with Co concentrations from $x = 0.3$ up to 0.45 by radio-frequency oxygen-plasma-assisted molecular beam epitaxy. The films retain their single crystalline wurtzite structure without any other crystallographic phase from precipitates, based on reflection high energy electron diffraction, X-ray diffraction, transmission electron microscopy, and Raman scattering. The results of X-ray diffraction, optical transmission spectroscopy, and in-situ X-ray photoelectron spectroscopy confirm the incorporation of Co^{2+} cations into the wurtzite lattice. The films exhibit robust ferromagnetism and the magneto-optical Kerr effect at room temperature. The saturation magnetization reaches 265 emu/cm^3 at $x = 0.45$, which corresponds to the average magnetic moment of 1.5 μ_B per Co atom. *Published by AIP Publishing*. [http://dx.doi.org/10.1063/1.4960555]

Ferromagnetic semiconductors have been attracting considerable attention for several decades because they combine two mainstream components of modern information technology, semiconductors for logic and magnetism for memory, within a single material. In particular, a ferromagnetic semiconductor with high Curie temperature (T_C) and large magnetization is highly desirable for practical applications of semiconductor spintronic devices that exploit both charge and spin to carry data.[1,2] Hence, extensive experimental searches have been performed via magnetic doping of various semiconducting materials, such as $Ga_{1-x}Mn_xAs$,[3] Mn_xGe_{1-x},[4] $Ti_{1-x}Co_xO_2$,[5] etc. Owing to the very low thermodynamic miscibility (typically $\le$10%) of transition metals (TMs) in semiconductors, however, high T_C ferromagnetic semiconductor research to date have been confined to dilute magnetic compounds containing minute amounts of magnetic ions. These are the so-called dilute magnetic semiconductors (DMSs). Despite considerable experimental efforts, the lack of high T_C and/or large magnetization has up to now impeded the application of DMS in practical spintronics devices.[6,7]

In order to realize high T_C and large magnetization in a semiconductor, the most direct way is to incorporate a higher concentration of magnetic ions by overcoming the obstacle represented by the low solid solubility of TM elements in semiconductors by means of non-equilibrium growth techniques. An extra high concentration ($\ge$30%) of magnetic ions must be introduced into the semiconductor matrix, substitutionally and uniformly. Moreover, the high dopant concentration should persist in the crystal structure of the semiconductor host in order to fit into current electronic techniques. Although a few research activities have been directed towards the development of heavily doping ferromagnetic semiconductors,[8–10] the technical realization of single phase semiconductor material with high concentration of magnetic dopants remains a challenge. In this work, we grew single crystalline wurtzite $Co_xZn_{1-x}O$ epitaxial films with Co concentrations from $x = 0.3$ up to 0.45 under conditions far from thermodynamic equilibrium. A systematic study of the structural, optical, and magnetic properties of the films is herein presented. The single crystalline wurtzite structure, robust ferromagnetism, and magneto-optical effect indicate the great potential of the $Co_xZn_{1-x}O$ films for practical spintronic devices operable at room temperature (RT).

The $Co_xZn_{1-x}O$ epitaxial films were grown on Al_2O_3 (0001) substrates by radio-frequency oxygen-plasma-assisted molecular beam epitaxy (RF-MBE). Metal fluxes were provided by evaporating high purity elemental solid sources (5N cobalt and 6N zinc). Oxygen flux was supplied in form of active oxygen (5N5) radicals by a radio-frequency plasma source. Before deposition, the Al_2O_3 substrates were thermally annealed at 800 °C for 10 min in the growth chamber with a base pressure of 1×10^{-9} mbar. A 40 nm ZnO buffer layer was first grown to relax the lattice mismatch, and then a $Co_xZn_{1-x}O$ epilayer 200 nm thick was deposited. During growth, $Co_xZn_{1-x}O$ epilayers were grown at the relatively

a)Authors to whom correspondence should be addressed. Electronic addresses: qiangcao@126.com and liu-guolei@sdu.edu.cn

low temperature of 400 °C, and the partial oxygen pressure was reduced to 10^{-7} mbar by using a liquid nitrogen trap. The film growth was monitored in real time by reflection high energy electron diffraction (RHEED). The Co concentration was manipulated by the flux ratio of Co and Zn, and cross-checked by energy dispersive x-ray analysis. The results of quantitative analysis are in good agreement with nominal compositions. The crystal structure of the films was characterized by high resolution XRD (Cu *Ka* radiation) and transmission electron microscopy (TEM). Non-resonant and resonant Raman measurements were carried out in backscattering geometry using an argon ion laser (488 nm) and a He–Cd laser (325 nm) as excitation sources, respectively. The optical transmission spectra were recorded using an ultraviolet (UV)-visible spectrometer in the energy range of 1–4 eV. The chemical composition and especially the oxidation state of Co in the epilayer were characterized by *in-situ* X-ray photoelectron spectroscopy (XPS). Longitudinal magneto-optical Kerr effect (MOKE) measurements were performed at RT using a He–Ne laser as light source with a wavelength of 632.8 nm. The *M-H* curves were measured by a superconducting quantum interference device (SQUID) from RT down to 5 K.

XRD patterns of the $Co_xZn_{1-x}O$ films with various Co concentrations are shown in Fig. 1(a). Besides the diffraction peak from the Al_2O_3 substrate, only (0002) and (0004) peaks of the hexagonal lattice were detected, indicating the single wurtzite structure of the films. The insets of Fig. 1(a) show the corresponding $[10\bar{1}0]$ RHEED patterns. No polycrystalline rings or surface structure other than hexagonal lattice are detected. The change from relatively streaky patterns to spotty patterns indicates that the surfaces of the films become rougher with increasing Co concentration. XRD ϕ-scans were performed to verify the single crystallinity of the $Co_xZn_{1-x}O$ films. As shown in Fig. 1(b), the sixfold symmetry of hexagonal structure is clearly revealed by six peaks separated by 60°, which demonstrates that the $Co_xZn_{1-x}O$ films are single domain epitaxial films without other orientations. The evolution of the lattice parameters *a*/*b* and *c* for the $Co_xZn_{1-x}O$ with various Co concentrations shows a close behaviour to Vegard's law.[12] As shown in Fig. 1(c), *c* increases with increasing Co concentration, whereas *a*/*b* decreases, indicating that Zn atoms are replaced by Co atoms. Otherwise, if Co atoms are in interstitial sites, both *a*/*b* and *c* will increase. The slight deviation from Vegard's law for higher Co concentration can be attributed to more lattice defects introduced by increasing Co concentration. The microscale and atomic structures of the films were investigated by TEM. A low-magnification TEM image is shown in Fig. 1(d), and the inset shows a representative cross-sectional high-resolution TEM image. The total thickness of the $Co_{0.45}Zn_{0.55}O$ film is about 200 nm. No phase segregation or Co-rich precipitates are found. Overall, the experimental results indicate that the $Co_xZn_{1-x}O$ films retain the single crystalline wurtzite structure with Co concentration *x* from 0.3 up to 0.45.

Non-resonant Raman spectra of the $Co_xZn_{1-x}O$ films with various Co concentrations are shown in Fig. 2(a). Besides the mode of the sapphire substrate at 750 cm^{-1}, three other Raman peaks are observed at 437, 576, and 240 cm^{-1}, respectively. According to the Raman selection rules in the wurtzite crystal structure, the modes at 437 and 576 cm^{-1} are separately assigned to the E_2 high frequency branch (E_{2H}) and A_1 longitudinal optical (LO) mode, respectively. Neither of the modes is shifted with increasing Co concentration. An additional mode around 240 cm^{-1} has also been reported for Mn doped ZnO,[13,14] manifesting it is not an element sensitive mode. The intensity of this peak increased with Mn concentration and decreased after annealing,[10] which indicates that the mode is probably related to damage or disorder of the crystal lattice induced by doping. The damage to the crystal lattice disrupts the long-range ordering in the ZnO crystal and

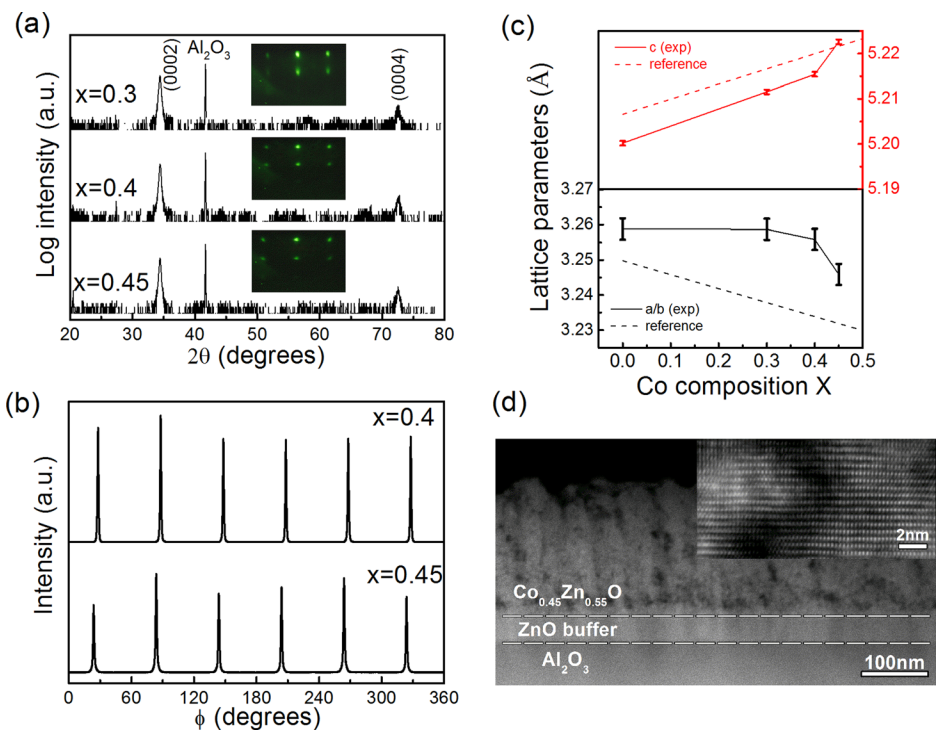

FIG. 1. (a) XRD and corresponding RHEED patterns of the $Co_xZn_{1-x}O$ films with $x = 0.3$, 0.4, and 0.45, respectively. (b) $(10\bar{1}2)$ ϕ-scans of $Co_{0.4}Zn_{0.6}O$ and $Co_{0.45}Zn_{0.55}O$ films. (c) Experimentally (exp) determined lattice parameters of *a*/*b* and *c* for the $Co_xZn_{1-x}O$ films with various Co concentrations. The dashed lines are plotted with lattice parameters taken from the reference standards of bulk ZnO and wurtzite CoO.[11] (d) Cross-sectional high-angle annular dark field scanning TEM image of $Co_{0.45}Zn_{0.55}O$ film. The inset shows a high-resolution TEM image of the same film.

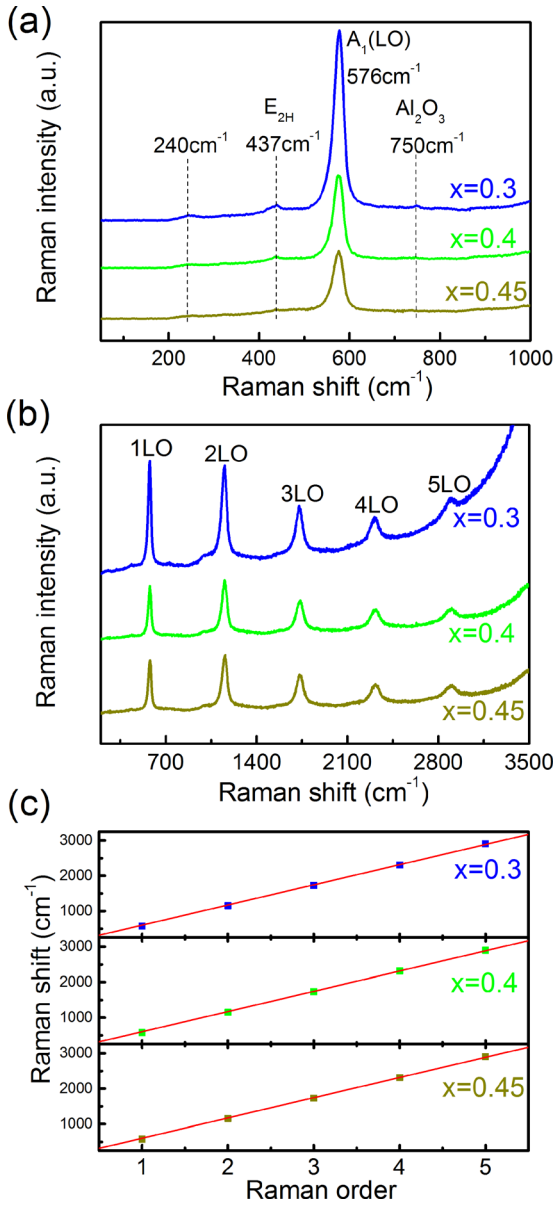

FIG. 2. (a) Non-resonant Raman spectra and (b) resonant Raman spectra for the $Co_xZn_{1-x}O$ films with $x = 0.3$, 0.4, and 0.45, respectively. (c) The positions of the resonant Raman modes as a function of order number, with the fits to the harmonic approximation shown by the solid lines.

causes the disorder-activated Raman scattering observed in the Brillouin zone. Therefore, the mode around 240 cm^{-1} is assigned to the acoustic-phonon branch at the zone boundary. It is worth mentioning that we do not observe any peaks related to segregated secondary phases such as Co clusters,[15,16] CoO,[17,18] Co_3O_4,[19,20] or $Zn_yCo_{3-y}O_4$.[20–22] In addition, the intensity of all the modes decreases with increasing Co concentration, which is due to radiative absorption by Co^{2+} color centers in the $Co_xZn_{1-x}O$ films with very high Co concentration.

Figure 2(b) shows resonant Raman spectra of the $Co_xZn_{1-x}O$ films. Multiple high-order Raman modes are clearly visible up to the fifth order for all the films. The first LO-phonon mode centered at 576 cm^{-1} is consistent with that observed in non-resonant spectra. The peak positions of the LO phonon and its overtones are hardly shifted at all as the Co concentration increases. Since resonant Raman spectroscopy can reveal high-order optical phonon modes, we are able to probe the crystal potential. In a simple harmonic oscillator, the energy levels are spaced equally: $E_{m+1} - E_m = \hbar\omega$, where ω is the oscillation frequency, and E_m and E_{m+1} are adjacent energy levels. For a multi-order Raman spectrum, the resonant LO Raman modes are positioned according to[23,24] $\omega_s^{(n)} = \omega_L - n\omega_{LO}$, where $\omega_s^{(n)}$ is the frequency of the nth-order LO Raman mode, ω_L is the frequency of the incident laser photon, n is the order number, and ω_{LO} is the LO phonon frequency. As shown in Fig. 2(c), the modes for all $Co_xZn_{1-x}O$ films follow the harmonic model closely and show little deviation up to the fifth order at ambient pressure, indicating harmonic phonon behavior similar to that in other reported hexagonal crystals such as ZnO,[25] $Zn_xCd_{1-x}Se$,[26] and CdS.[27]

Figure 3(a) shows the optical transmission spectra for ZnO and $Co_xZn_{1-x}O$ films. Pure ZnO film is fully transparent in the visible light region, and the energy band gap is 3.32 eV. The extra optical signal above the energy of the band gap is due to fluorescence of the Al_2O_3 substrate, which is invisible in the ZnO films grown on $SrTiO_3$ substrate under the same growth conditions. In the case of the $Co_xZn_{1-x}O$ films, the transmittance maxima decrease significantly with increasing Co concentration. The films are still semitransparent in the visible light region, however, and the transmittance decreases with increasing excitation photon energy. Three characteristic absorptions are observed at 1.86, 2.01, and 2.17 eV, which are indicated by the arrows in Fig. 3(a). They are correlated with the *d-d* transitions of Co^{2+} ions with the $3d^7$ high-spin configuration in a tetrahedral crystal field formed by neighboring O^{2-} ions,[28–30] which indicates the substitutional replacement of tetrahedrally coordinated Zn ions.

The oxidation states of Co in the $Co_xZn_{1-x}O$ films were characterized by *in-situ* XPS spectra. Co metal clusters near the film surface can be identified if they exist, since they cannot be oxidized to Co^{2+} without air exposure. As shown in Fig. 3(b), the XPS spectra of the $Co_xZn_{1-x}O$ films are in sharp contrast to those of Co metal or Co clusters. Their Co^{2+} character can be deduced from the presence of a satellite structure 5 eV above the Co $2p_{3/2}$ main line.[31] The difference in energy between the Co $2p_{3/2}$ and $2p_{1/2}$ peaks is about 15.5 eV, which also matches that for standard CoO,[31,32] indicating the divalent state of Co, as expected for substituted Co ions at Zn sites.

Figure 4(a) presents the temperature dependent hysteresis loops of the $Co_{0.3}Zn_{0.7}O$ film. When the films were cooled from 300 K to 5 K, the coercivity was enhanced from 232 Oe to 740 Oe, but the increase in the saturated magnetization (M_s) was very slight from 38 emu/cm^3 at 300 K to 41 emu/cm^3 at 5 K. The long range ferromagnetic order is dominant in our $Co_xZn_{1-x}O$ films at RT.

Furthermore, the $Co_xZn_{1-x}O$ films exhibit stronger magneto-optic properties, as revealed by the MOKE spectra. The hysteresis measured from the MOKE spectra at RT for $Co_{0.4}Zn_{0.6}O$ film is shown in Fig. 4(b). For comparison, magnetization data measured for the same film using a SQUID are also included. The SQUID and MOKE hysteresis results are in excellent agreement. In addition, obvious magnetic anisotropy with the hard axis perpendicular to the film is

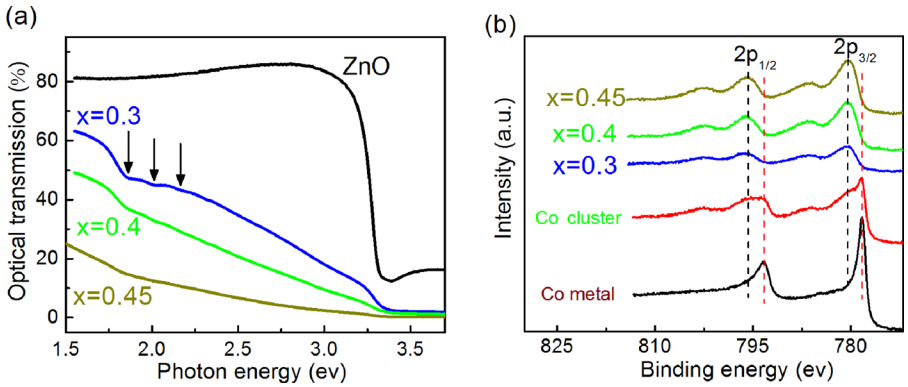

FIG. 3. (a) Optical transmission and (b) in-situ XPS spectra of Co $2p_{1/2,\ 3/2}$ for the $Co_xZn_{1-x}O$ films with $x = 0.3$, 0.4, and 0.45, respectively. The spectra of Co metal and Co metal clusters embedded in ZnO are also shown for comparison.

shown in Fig. 4(c), indicating a continuous magnetic layer rather than a magnetic granular film or magnetic clusters embedded in a ZnO matrix. As shown in Figs. 4(a)–4(c), the M_s and remnant magnetization are both remarkably enhanced with increasing Co concentration. M_s reaches 265 emu/cm^3 at $x = 0.45$. Assuming that the magnetic moments purely come from Co atoms, the average magnetic moment is 1.5 μ_B per Co for the $Co_{0.45}Zn_{0.55}O$ film at RT. It is worth to mention that there is no deterioration of magnetic moment with time at least for one year, indicating a stable ferromagnetism for our films. Moreover, the resistivity of $Co_xZn_{1-x}O$ films increases with decreasing temperature from RT down to 5 K, showing a clear semiconducting, rather than metallic character.

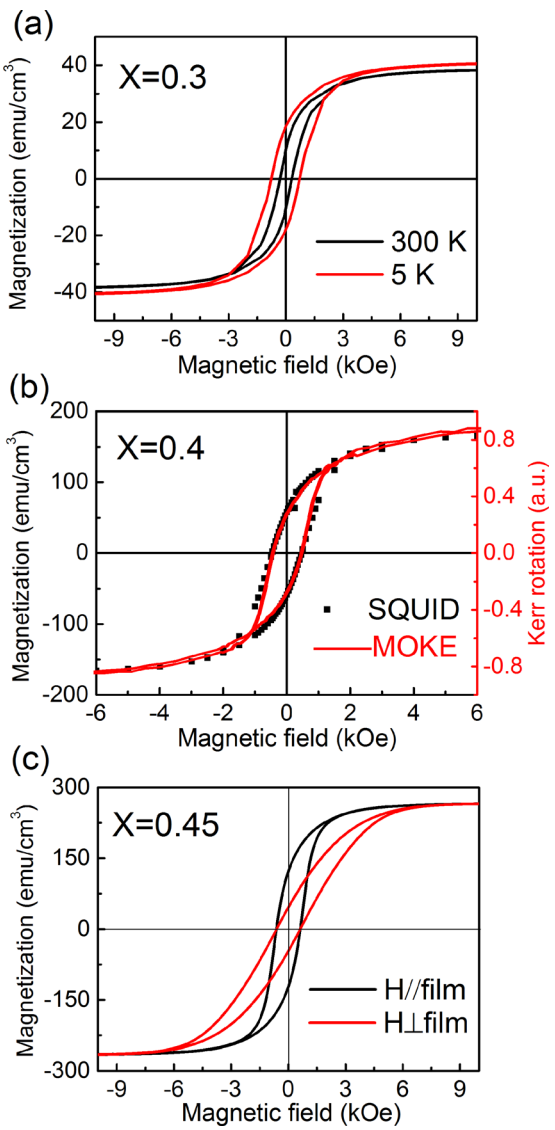

FIG. 4. (a) Magnetic hysteresis loops of $Co_{0.3}Zn_{0.7}O$ film at RT and 5 K. (b) RT magnetic hysteresis loops measured for $Co_{0.4}Zn_{0.6}O$ film from SQUID magnetization data (closed blocks) are superimposed on the MOKE data (red line). (c) Magnetic anisotropy of $Co_{0.45}Zn_{0.55}O$ film at RT.

In summary, we have grown single crystalline $Co_xZn_{1-x}O$ epitaxial films with high Co concentration by RF-MBE. The films retain their single crystalline wurtzite structure with Co concentrations from x = 0.3 up to 0.45. No phase segregation or Co-rich precipitates are found. The films exhibit robust ferromagnetism and the magneto-optical Kerr effect at RT. The saturation magnetization reaches 265 emu/cm^3 at $x = 0.45$, which corresponds to an average magnetic moment of 1.5 μ_B per Co atom. As an alternative to conventional diluted magnetic semiconductor, the approach of growing single crystalline semiconductor films with a high concentration of magnetic atoms opens up a dimension in the search for ferromagnetic semiconductors that work at RT.

This work was supported by the State Key Project of Fundamental Research of China under Grant Nos. 2013CB922303 and 2015CB921400, the NSFC for Distinguished Young Scholar No. 51125004, the NSF Grant Nos. 11374189 and 51231007, 111 project B13029. P.Y. was supported by the SSLS via NUS Core Support C-380-003-003-001.

[1]A. H. MacDonald, P. Schiffer, and N. Samarth, Nat. Mater. **4**, 195 (2005).
[2]K. Ando, Science **312**, 1883 (2006).
[3]H. Ohno, A. Shen, F. Matsukura, A. Oiwa, A. Endo, S. Katsumoto, and Y. Iye, Appl. Phys. Lett. **69**, 363 (1996).
[4]Y. D. Park, A. T. Hanbicki, S. C. Erwin, C. S. Hellberg, J. M. Sullivan, J. E. Mattson, T. F. Ambrose, A. Wilson, G. Spanos, and B. T. Jonker, Science **295**, 651 (2002).
[5]Y. Matsumoto, M. Murakami, T. Shono, T. Hasegawa, T. Fukumura, M. Kawasaki, P. Ahmet, T. Chikyow, S. Koshihara, and H. Koinuma, Science **291**, 854 (2001).
[6]T. Dietl and H. Ohno, Rev. Mod. Phys. **86**, 187 (2014).
[7]S. B. Ogale, Adv. Mater. **22**, 3125 (2010).
[8]Y. J. Zeng, N. Gauquelin, D. Y. Li, S. C. Ruan, H. P. He, R. Egoavil, Z. Z. Ye, J. Verbeeck, J. Hadermann, M. J. Van Bael, and C. Van Haesendonck, ACS Appl. Mater. Interfaces **7**, 22166 (2015).
[9]K. Akaiwa, K. Kaneko, S. Fujita, E. Chikoidze, and Y. Dumont, Appl. Phys. Lett. **106**, 062405 (2015).
[10]N. T. Tu, P. N. Hai, L. D. Anh, and M. Tanaka, Phys. Rev. B **92**, 144403 (2015).

[11]M. J. Redman and E. G. Steward, Nature **193**, 867 (1962).
[12]A. R. Denton and N. W. Ashcroft, Phys. Rev. A **43**, 3161 (1991).
[13]J. B. Wang, H. M. Zhong, Z. F. Li, and W. Lu, Appl. Phys. Lett. **88**, 101913 (2006).
[14]H. Zhong, J. Wang, X. Chen, Z. Li, W. Xu, and W. Lu, J. Appl. Phys. **99**, 103905 (2006).
[15]M. Millot, J. Gonzalez, I. Molina, B. Salas, Z. Golacki, J. M. Broto, H. Rakoto, and M. Goiran, J. Alloys Compd. **423**, 224 (2006).
[16]W. Szuszkiewicza, J. F. Morhangeb, Z. Golackia, A. Lusakowskia, M. Schummc, and J. Geurtsc, Acta Phys. Pol., A **112**, 363 (2007).
[17]H. Chou and H. Fan, Phys. Rev. B **13**, 3924 (1976).
[18]D. Gallant, M. Pézolet, and S. Simard, J. Phys. Chem. B **110**, 6871 (2006).
[19]X. Wang, J. Xu, X. Yu, K. Xue, J. Yu, and X. Zhao, Appl. Phys. Lett. **91**, 031908 (2007).
[20]V. G. Hadjiev, M. N. Iliev, and I. V. Vergilov, J. Phys. C: Solid State Phys. **21**, L199 (1988).
[21]M. Schumm, M. Koerdel, S. Muller, C. Ronning, E. Dynowska, Z. Gołacki, W. Szuszkiewicz, and J. Geurts, J. Appl. Phys. **105**, 083525 (2009).
[22]K. Samanta, P. Bhattacharya, R. Katiyar, W. Iwamoto, P. Pagliuso, and C. Rettori, Phys. Rev. B **73**, 245213 (2006).
[23]J. F. Scott, T. C. Damen, W. T. Silfvast, R. C. C. Leite, and L. E. Cheesman, Opt. Commun. **1**, 397 (1970).
[24]J. F. Kong, W. Z. Shen, Y. W. Zhang, C. Yang, and X. M. Li, Appl. Phys. Lett. **92**, 191910 (2008).
[25]J. F. Scott, Phys. Rev. B **2**, 1209 (1970).
[26]W. S. Li, Z. X. Shen, D. Z. Shen, and X. W. Fan, J. Appl. Phys. **84**, 5198 (1998).
[27]I. H. Choi and P. Y. Yu, Phys. Status Solidi B **242**, 2813 (2005).
[28]S. Ramachandran, A. Tiwari, and J. Narayan, Appl. Phys. Lett. **84**, 5255 (2004).
[29]P. Koidl, Phys. Rev. B **15**, 2493 (1977).
[30]M. Bouloudenine, N. Viart, S. Colis, J. Kortus, and A. Dinia, Appl. Phys. Lett. **87**, 052501 (2005).
[31]J. F. Moulder, W. F. Stickle, P. E. Sobol, and K. D. Bomben, *Hand-Book of X-ray Photoelectron Spectroscopy*, edited by J. Chastain (Perkin Elmer, Eden Prairie, MN, 1992), p. 83.
[32]C. C. Wang, B. Y. Man, M. Liu, C. S. Chen, S. Z. Jiang, S. Y. Yang, S. C. Xu, X. G. Gao, and B. Hu, Adv. Condens. Matter Phys. **2012**, 1.